26th EPS Conf. on Contr. Fusion and Plasma Physics, Maastricht, 14 - 18 June 1999 ECA Vol.23J (1999) 481 - 484

Numerical Study of Chaos Based on a Shell Model

M. Yagi, S.-I. Itoh, K. Itoh*, A. Fukuyama†

Research Institute for Applied Mechanics, Kyushu University, Kasuga 816-8580
** National Institute for Fusion Science, Toki, 509-5292, Japan*
† Faculty of Engineering, Kyoto University, Kyoto 606-8501

Abstract

A shell model is introduced to study a turbulence driven by the thermal instability (interchange mode with $k_{\|} = 0$, and/or Rayleigh-Bénard convection in neutral fluids). This model equation describes cascade and chaos in the strong turbulence with high Rayleigh number. The chaos is numerically studied based on this model. The characteristics of the turbulence are analyzed in respect of Rayleigh number and Prandtl number.

1. Introduction

Recently, the extended Lorenz model was proposed as the model describing the dynamics of Scrape Off Layer (SOL) in tokamak plasmas[1]. Such a model has also been applied to Edge Localized Modes (ELMs) which are observed during high confinement mode (H-mode). However, it is found that a model with a few degrees of freedom is not relevant to describe the dynamics in high Rayleigh number regime. Such a model only shows a limit cycle in high Rayleigh number limit[2]. Here we propose a shell model which is relevant to study a turbulence driven by interchange mode or Rayleigh-Bénard instability[3]. This model equation describes cascade and chaos in the strong turbulence with high Rayleigh number. The chaos is numerically studied based on this model. Statistical quantities (such as a mean value of total energy, it's standard deviation, time averaged wave spectrum, frequency spectrum, an instantaneous maximum Lyapunov exponent) are evaluated.

2 Model and Basic Equations

We extend the Gledzer-Ohkitani-Yamada (GOY) model[4] to describe the thermal instability (interchange mode or Rayleigh-Bénard convection). The extended model (Yagi model) retains only one complex mode as a representative of all the Fourier modes in the shell of wave numbers between octave and only nonlinear couplings to the next nearest shell are kept. Basic equations are written as

$$\frac{du_n}{dt} = i(a_n u^*_{n+1}u^*_{n+2} + b_n u^*_{n-1}u^*_{n+1} + c_n u^*_{n-1}u^*_{n-2}) + P_r\theta_n - P_r k_n^2 u_n \qquad (1)$$

$$\frac{d\theta_n}{dt} = i\{e_n(u^*_{n-1}\theta^*_{n+1} - u^*_{n+1}\theta^*_{n-1}) + g_n(u^*_{n-2}\theta^*_{n-1} + u^*_{n-1}\theta^*_{n-2}) + h_n(u^*_{n+1}\theta^*_{n+2} + u^*_{n+2}\theta^*_{n+1}) + R_a u_n - k_n^2\theta_n \qquad (2)$$

where * represents the complex conjugate, $n = 1,\cdots,N$, number of each shell, u_n, the fluctuating velocity, θ_n, the fluctuating temperature, $k_n = C2^{n-1}$, the wavenumber, P_r, the Prandtl number, R_a, the Rayleigh number. In this model, each shell k_n consists of the wave numbers k such that $k_{n-1} < k < k_n$. The Fourier transform of the velocity difference over a length scale $\simeq k_n^{-1}$ is given by a corresponding complex variables u_n, i.e.,

$$|u_n|^2 = \int_{k_{n-1}}^{k_n} |v(k)|^2 dk \qquad (3)$$

where $v(k)$ is the velocity field. For the boundary conditions, we assume $u_0 = u_{N+1} = 0$ and $\theta_0 = \theta_{N+1} = 0$. The coefficients are given by

$$a_n = k_n,\ b_n = -\frac{k_{n-1}}{2},\ c_n = -\frac{k_{n-2}}{2},\ e_n = \frac{k_n}{2},\ g_n = -\frac{k_{n-1}}{2},\ h_n = \frac{k_{n+1}}{2}, \quad (4)$$

and

$$b_1 = b_N = c_1 = c_2 = a_{N-1} = a_N = e_1 = e_N = g_1 = g_2 = h_{N-1} = h_N = 0. \quad (5)$$

Here the typical scale length L and the thermal diffusion time $L^2\kappa^{-1}$ (κ molecular thermal conductivity) are used for normalization[5].

Next, we briefly show the characteristics of this model. This model contains the linear thermal instability. The linear growth rate γ_n is estimated by

$$\gamma_n = \frac{-k_n^2(1+P_r) + \sqrt{k_n^4(1-P_r)^2 + 4P_r R_a}}{2}. \quad (6)$$

The n-th mode becomes linearly unstable if $R_a > k_n^4$ holds. The threshold value for the linear instability to exist is given by $R_{ac} = k_1^4$. This model also has a self-similar solution

$$u_n = A\, k_n^{-1/3},\ \theta_n = \sqrt{R_a} u_n \quad (7)$$

where A is a complex constant. The relation $u_n \propto k_n^{-1/3}$ implies the inertia-range scaling $|v(k)|^2 \propto k^{-5/3}$ [6]. This result shows that the model equation describes the spectrum cascade in the presence of instability.

3. Numerical Analysis and Characteristics of the Model

The following parameters are used for numerical simulations; $C = 1$ and the numbers of shells $N = 13$ for $R_a = 2\times10^4$, $N = 14$ for $R_a = 10^6, 10^7$.

(a) Time averaged wavenumber spectrum

Figure 1 shows the log-log plot of the time averaged wavenumber spectra of u_n and θ_n in the case of $R_a = 2\times10^4$ and $P_r = 1$. The circle corresponds to the spectrum of u_n, the triangles correspond to the spectrum of θ_n, respectively. Time averaging is performed from $t = 0.2$ to $t = 10.0$. In the wavenumber region, $2 \le k_n \le 16$, both variables, as averages, obey the scaling law, $u_n \propto k_n^{-1/3}$ and $\theta_n \sim k_n^{-1/3}$ as are shown by the dotted lines. They fluctuate around the line proportional to $k_n^{-1/3}$.

(b) Total energy

Firstly, we investigate the Rayleigh number dependence of the saturation level of total energy. Figure 2 shows the time evolution of total energy $E(t)$ in the case of $P_r = 1$. The solid line corresponds to the case of $R_a = 2\times10^4$. The dotted-dashed line shows the case of $R_a = 10^6$ and the dotted line shows the case of $R_a = 10^7$. Here, the total energy is defined by

$$E(t) = \frac{1}{2}\sum_n \left(|u_n|^2 + |\theta_n|^2 \right). \quad (8)$$

The total energy tends to saturate in the nonlinear phase, however, the fluctuation around the mean value of the total energy is observed, which shows the chaotic nature of the system. Both the mean value and the fluctuation amplitude increases with the Rayleigh number. This is because the saturation level of the total energy is roughly determined by the maximum linear growth rate and the nonlinear dumping rate.

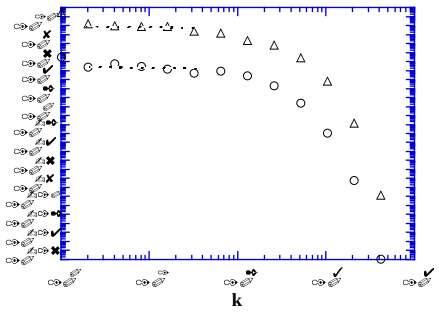

Fig.1 The time averaged wavenumber spectra.

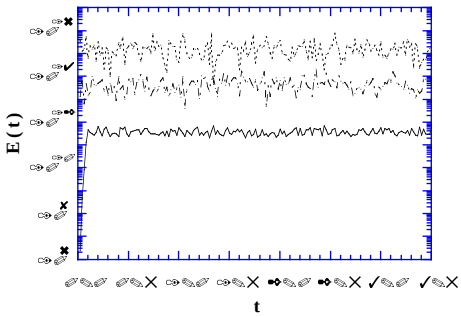

Fig.2 The time evolution of total energy for various values of Rayleigh number.

Next, we investigate the Prandtl number dependence of the saturation level of total energy. Figure 3 shows the time evolution of the total energy in the case of $R_a = 2 \times 10^4$. The solid line corresponds to the case of $P_r = 2$, the dotted-dashed line is the case of $P_r = 5$ and the dotted line shows the case of $P_r = 8$. The total energy also fluctuates as is observed in fig.2. In contrast to the Rayleigh number dependence, the fluctuation amplitude relative to the mean value of the total energy is found to decrease as the Prandtl number increases. The increase of the mean saturation level with the increase of Prandtl number is correlated with the maximum linear growth rate as is the case of the Rayleigh number dependence.

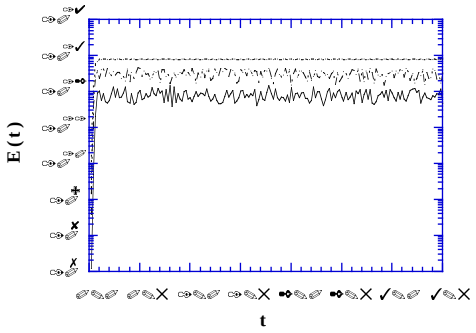

Fig.3 The time evolution of total energy for various values of Prandtl number.

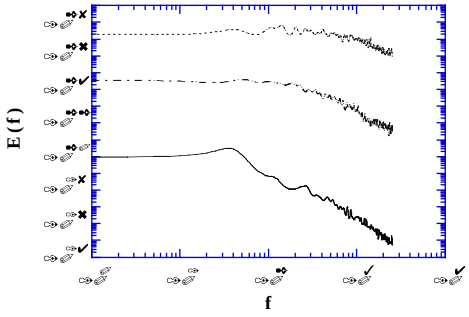

Fig.4 The power spectrum of the total energy for various values of Rayleigh number.

(c) Power spectrum of total energy

Figure 4 shows the log-log plot of the power spectrum of the total energy with $P_r = 1$ for various values of Rayleigh number. The frequency is defined as $f = (j-1)\,\Delta f$, $(j = 1,2,\cdots)$ where $\Delta f = 2.5$. The solid line shows the power spectrum for $R_a = 2 \times 10^4$, the dotted-dashed line is the case of $R_a = 10^6$ and the dotted line corresponds to the case of $R_a = 10^7$. Continuous spectra are obtained in these cases. For $R_a = 2 \times 10^4$, $R_a = 10^6$ and $R_a = 10^7$, the power spectra are fitted as $E(f) \sim f^{-3.88}$, $E(f) \sim f^{-2.45}$ and $E(f) \sim f^{-2.25}$ in $1000 < f < 2500$, respectively.

Figure 5 shows the log-log plot of the power spectrum of the total energy with $R_a = 2 \times 10^4$ for different values of Prandtl number, corresponding to those in Fig.3. The solid line corresponds to the case of $P_r = 2$, the dotted-dashed line is the case of $P_r = 5$ and the dotted line to the case of $P_r = 8$. For $P_r = 2$ and $P_r = 5$, the power spectra are fitted as $E(f) \sim f^{-3.15}$ and $E(f) \sim f^{-2.02}$, respectively in the range of $1000 < f < 2500$. On the otherhand, the fundamental and the harmonic frequencies are observed in the case of $P_r = 8$. This corresponds the fact that the amplitude of deviation is very small and converges to the limit cycle. To confirm this result, we also calculate the maximum Lyapunov exponents.

Figure 6 shows the plot of the maximum Lyapunov exponent versus the Prandtl number. It is found that the values of the maximum Lyapunov exponent are positive in the region, $0.5 \le P_r \le 7.5$ and almost zero in the region, $8 \le P_r \le 10$. We conclude that both parameters, R_a and P_r have the destabilizing effect on the linear mode, which reflects to the mean value of saturation amplitude. The Rayleigh number has an effect of destabilizing on the nonlinear mode, while, the Prandtl number has an effects of both stabilizing and destabilizing on the nonlinear mode in these parameter regime. (The transition from turbulence to ordered motion at high P_r has been reported experimentally [7].)

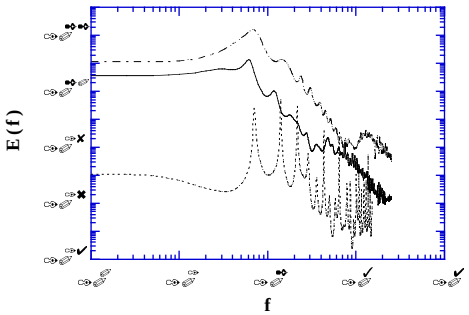

Fig.5 The power spectrum of the total energy for various values of Prandtl number.

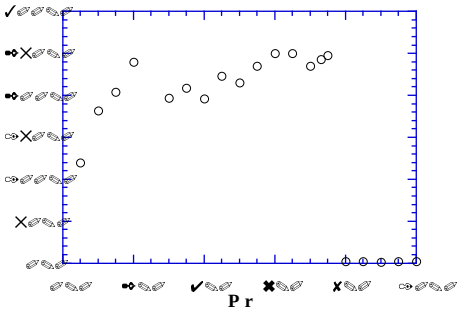

Fig.6 The maximum Lyapunov exponents for various values of Rayleigh number.

4. Summary and Discussion

In this article, a new shell model which is extended to describe a turbulence driven by the thermal instability is introduced and analyzed. Parameter survey is done with respect to the Rayleigh number and the Prandtl number. It is shown that this model contains a chaotic attractor and a limit cycle, the appearance depends on the Prandtl number.

Acknowledgements

This work is partly supported by the Grant-in-Aid for Scientific Research of Ministry of Education, Science, Sports and Culture of Japan, by the REIMEI Research Resources of the Japan Atomic Energy Research Institute and by the collaboration program of Advanced Fusion Research Center, RIAM of Kyushu University.

References

[1] O. Pogutse et al., Plasma Phys. Control. Fusion **36** 1963 (1994).
[2] T. Aoyagi, M. Yagi and S.-I. Itoh, J. Phys. Soc. Jpn **66** 2689 (1997).
[3] M. Yagi, S.-I. Itoh, K. Itoh and A. Fukuyama, Chaos **9** Issue 2 (1999) in press.
[4] M. Yamada and K. Ohkitani, J. Phys. Soc. Jpn. **56** 4210 (1987).
[5] P. Manneville, Dissipative Structures and Weak Turbulence, Academic Press Inc., P.55 (1990).
[6] A. N. Kolmogorov, Dokl. Akad. Nauk SSSR **30** 9 (1941), **31** 538 (1941), **32** 16 (1941), **31** 99 (1941).
[7] R. Krishunamulti, J. Fluid Mech. **42** 295 (1971).